Electronic Supplementary Material (ESI) for Physical Chemistry Chemical Physics.

Supporting Information

Orientation and Dynamics of Cu^{2+} Based DNA Label from Force Field Parameterized MD Elucidates the Relationship Between EPR Distance Constraints and DNA Backbone Distances

Shreya Ghosh[a], Joshua Casto[a], Xiaowei Bogetti[a], Charu Arora[a], Junmei Wang*[b] and Sunil Saxena*[a]

[a.] *Department of Chemistry, University of Pittsburgh, PA 15260, USA. Email: sksaxena@pitt.edu*
[b.] *Department of Pharmaceutical Sciences, University of Pittsburgh, PA 15206, USA. Email: junmei.wang@pitt.edu*

Force field parameters of Cu^{2+}-DPA and dSpacer

Residue Topology of Cu^{2+}-DPA-WAT_1

```
    0    0    2
This is a remark line
dpa.res
DPA   INT  0
CORRECT     OMIT DU   BEG
  0.0000
   1  DUMM  DU    M    0  -1  -2     0.000      .0        .0      .00000
   2  DUMM  DU    M    1   0  -1     1.449      .0        .0      .00000
   3  DUMM  DU    M    2   1   0     1.523   111.21       .0      .00000
   4  P2    P     M    3   2   1     1.540   111.208  -180.000  1.369015
   5  O6    O2    E    4   3   2     1.503   138.219  -132.370 -0.834137
   6  O7    O2    E    4   3   2     1.504    69.118   111.415 -0.834137
   7  O5    OS    M    4   3   2     1.666    41.750   -83.842 -0.434069
   8  C13   CT    M    7   4   3     1.423   117.834    24.136 -0.069712
   9  H20   H1    E    8   7   4     1.097   110.010   -66.592  0.048214
  10  H21   H1    E    8   7   4     1.098   110.806    53.014  0.048214
  11  C11   CT    M    8   7   4     1.529   108.550   172.648  0.523010
  12  C16   CT    3   11   8   7     1.537   108.764   164.916 -0.072228
  13  N1    N3    S   12  11   8     1.502   117.117   176.539  0.060271
  14  Cu1   Cu    3   13  12  11     2.010   102.855   163.593  0.930057
  15  N2    NX    S   14  13  12     1.966    84.525   -91.969 -0.533625
  16  C2    CA    B   15  14  13     1.354   112.881   -12.764  0.418204
  17  C1    CT    B   16  15  14     1.508   115.313    -6.306 -0.382868
  18  H1    HP    E   17  16  15     1.096   108.214   -86.447  0.166229
  19  H2    HP    E   17  16  15     1.096   112.326   155.202  0.166229
  20  C3    CA    B   16  15  14     1.390   121.578   176.281 -0.248187
  21  H3    HA    E   20  16  15     1.084   119.664  -179.204  0.194440
  22  C4    CA    B   20  16  15     1.395   118.963     0.690  0.058679
  23  H4    HA    E   22  20  16     1.085   120.170   179.937  0.169276
  24  C5    CA    B   22  20  16     1.395   119.256    -0.439 -0.273038
  25  H5    HA    E   24  22  20     1.084   121.597  -179.698  0.185970
  26  C6    CA    S   24  22  20     1.389   118.706    -0.256  0.188894
  27  H6    H4    E   26  24  22     1.082   121.359  -179.268  0.067462
  28  N3    NZ    S   14  13  12     1.959    84.734    94.839 -0.533625
  29  C8    CA    B   28  14  13     1.353   113.489    10.902  0.418204
  30  C7    CT    B   29  28  14     1.509   115.858     5.706 -0.382868
  31  H7    HP    E   30  29  28     1.090   112.312  -149.878  0.166229
  32  H8    HP    E   30  29  28     1.095   108.521    91.444  0.166229
  33  C9    CA    B   29  28  14     1.391   121.329  -176.852 -0.248187
  34  H9    HA    E   33  29  28     1.085   119.725   179.384  0.194440
  35  C10   CA    B   33  29  28     1.394   119.024    -0.668  0.058679
  36  C14   CA    B   35  33  29     1.395   119.252     0.461 -0.273038
  37  H10   HA    E   36  35  33     1.084   121.472   179.710  0.185970
  38  C15   CA    S   36  35  33     1.388   118.813     0.200  0.188894
  39  H11   H4    E   38  36  35     1.082   122.105   179.267  0.067462
  40  H22   HA    E   35  33  29     1.085   120.171  -179.944  0.169276
  41  O9    ow    B   14  13  12     2.017   169.111    13.639 -0.592041
  42  H18   hw    E   41  14  13     0.973   121.699  -173.567  0.414588
  43  H19   hw    E   41  14  13     0.972   120.565   -33.308  0.414588
  44  H24   HP    E   12  11   8     1.094   107.367   -62.153  0.030515
  45  H25   HP    E   12  11   8     1.094   110.203    54.612  0.030515
```

```
  46  H23   H1    E   11   8   7     1.093   108.135    45.383  0.020529
  47  O1    OS    M   11   8   7     1.427   109.983   -73.869 -0.408523
LOOP
   C1   N1
   C7   N1
   C6   N2
  C15   N3
IMPROPER
   C2   C6   N2  Cu1
   C3   C1   C2   N2
   C2   C4   C3   H3
   C3   C5   C4   H4
   C4   C6   C5   H5
   C5   H6   C6   N2
   C8  C15   N3  Cu1
   C9   C7   C8   N3
   C8  C10   C9   H9
   C9  C14  C10  H22
  C10  C15  C14  H10
  C14  H11  C15   N3
DONE
STOP
```

Residue Topology of dSpacer

```
    0    0    2
This is a remark line
DSP.res
DSP   INT  0
CORRECT     OMIT DU   BEG
  0.0000
   1  DUMM  DU    M    0  -1  -2     0.000      .0        .0      .00000
   2  DUMM  DU    M    1   0  -1     1.449      .0        .0      .00000
   3  DUMM  DU    M    2   1   0     1.523   111.21       .0      .00000
   4  P2    P     M   3   2   1      1.540   111.208  -180.000  1.295965
   5  O4    O2    E   4   3   2      1.473    54.315   -77.788 -0.826887
   6  O6    O2    E   4   3   2      1.478    93.607    49.757 -0.826887
   7  O3    OS    M   4   3   2      1.619   155.989  -126.296 -0.522060
   8  C5    CT    M   7   4   3      1.401   120.164  -146.267  0.096810
   9  H4    H1    E   8   7   4      1.085   109.662   -60.978  0.033214
  10  H5    H1    E   8   7   4      1.086   110.081    57.875  0.033214
  11  C1    CT    M   8   7   4      1.521   109.828   178.845  0.389113
  12  O1    OS    S   11  8   7      1.420   110.213   -63.586 -0.523884
  13  C4    CT    3   12  11  8      1.403   110.936  -121.973  0.146514
  14  C3    CT    B   13  12  11     1.521   105.399    23.279 -0.038815
  15  H9    HC    E   14  13  12     1.087   110.254    79.352  0.013253
  16  H10   HC    E   14  13  12     1.081   113.757  -157.319  0.013253
  17  H2    H1    E   13  12  11     1.086   108.288   145.251  0.027202
  18  H3    H1    E   13  12  11     1.086   110.563   -96.056  0.027202
  19  H1    H1    E   11  8   7      1.082   109.213    55.803  0.019398
  20  C2    CT    M   11  8   7      1.539   112.747   178.156  0.161221
  21  H14   H1    E   20  11  8      1.081   112.923   -24.157  0.031635
  22  O9    OS    M   20  11  8      1.408   108.473  -145.576 -0.549462
LOOP
```

```
   C2   C3
IMPROPER
DONE
STOP
```

Key Force Field Parameters of Cu^{2+}-DPA-WAT_1

```
Remark line goes here
MASS
Cu 63.010        0.000
NX 14.010        0.530              same as nc
NZ 14.010        0.530              same as nc
hw 1.008         0.000              H in TIP3P water
ow 16.00         0.000              oxygen in TIP3P water
BOND
Cu-N3   47.11   2.010       calculated for Cu-N3
Cu-NX   52.79   1.966       calculated for Cu-NX
Cu-NZ   53.77   1.959       calculated for Cu-NZ
Cu-ow   39.51   2.017       calculated for Cu-OX
CA-NX  394.60   1.352       same as ca-nc, penalty score=  0.0
CA-NZ  394.60   1.352       same as ca-nc, penalty score=  0.0
ow-hw  553.0    0.9572    ! TIP3P water
hw-hw  553.0    1.5136      TIP3P water
ANGLE
CT-N3-Cu   20.541     105.102
N3-Cu-NX   45.470      84.527
N3-Cu-NZ   45.491      84.734
N3-Cu-ow   31.748     169.109
NX-Cu-NZ   32.749     167.291
NX-Cu-ow   42.088      98.298
NZ-Cu-ow   43.223      93.513
CA-NX-Cu   19.811     120.227
CA-NZ-Cu   19.891     120.080
Cu-ow-hw   11.709     121.130
CA-CT-N3   81.700     113.800
CT-CA-NX   85.113     115.317
CA-CA-NX   87.600     119.720
H4-CA-NX   63.000     118.360
CA-NX-CA   72.000     109.950
CA-CT-HP   47.300     110.470
CT-CA-NZ   84.914     115.858
CA-CA-NZ   87.600     119.720
H4-CA-NZ   63.000     118.360
CA-NZ-CA   72.000     109.950
hw-ow-hw    100.      104.52
hw-hw-ow      0.      127.74
DIHE
NX-Cu-N3-CT   1    0.000         0.000          2.000
NZ-Cu-N3-CT   1    0.000         0.000          2.000
ow-Cu-N3-CT   1    0.000         0.000          2.000
N3-Cu-NX-CA   1    0.000         0.000          2.000
N3-Cu-NZ-CA   1    0.000         0.000          2.000
N3-Cu-ow-hw   1    0.000         0.000          2.000
CT-CA-NX-Cu   2    9.600       180.000          2.000
```

```
CA-CA-NX-Cu   2    9.600       180.000          2.000
H4-CA-NX-Cu   2    9.600       180.000          2.000
CT-CA-NZ-Cu   2    9.600       180.000          2.000
CA-CA-NZ-Cu   2    9.600       180.000          2.000
H4-CA-NZ-Cu   2    9.600       180.000          2.000
NX-Cu-NZ-CA   1    0.000         0.000          2.000
NX-Cu-ow-hw   1    0.000         0.000          2.000
CA-CA-NX-CA   2    9.600       180.000          2.000
H4-CA-NX-CA   2    9.600       180.000          2.000
CT-CA-NX-CA   2    9.600       180.000          2.000
NZ-Cu-NX-CA   1    0.000         0.000          2.000
NZ-Cu-ow-hw   1    0.000         0.000          2.000
CA-CA-NZ-CA   2    9.600       180.000          2.000
H4-CA-NZ-CA   2    9.600       180.000          2.000
CT-CA-NZ-CA   2    9.600       180.000          2.000
ow-Cu-NX-CA   1    0.000         0.000          2.000
ow-Cu-NZ-CA   1    0.000         0.000          2.000
hw-hw-ow-Cu   1    0.000         0.000          2.000
IMPROPER
CA-CA-NX-Cu          1.1          180.0         2.0
CA-CT-CA-NX          1.1          180.0         2.0
CA-CA-CA-HA          1.1          180.0         2.0
CA-H4-CA-NX          1.1          180.0         2.0
CA-CA-NZ-Cu          1.1          180.0         2.0
CA-CT-CA-NZ          1.1          180.0         2.0
CA-H4-CA-NZ          1.1          180.0         2.0
NONBON
  Cu          2.2100  0.1729
  NX          1.8993  0.0941
  NZ          1.8993  0.0941
  ow          1.8200  0.0930
  hw          0.3019  0.0047
```

Comparison of distance distribution from MD simulations and experiment

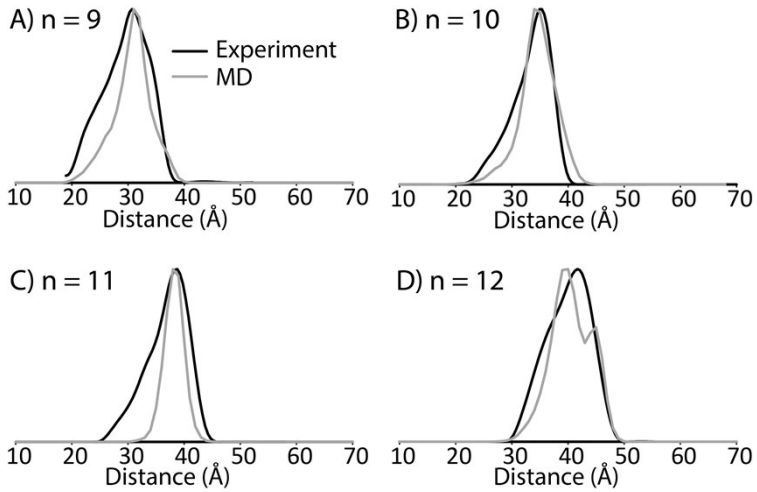

Figure S1: Cu^{2+}-Cu^{2+} distance distribution from 2 μs MD simulations (grey) and experiment (black) for duplexes with base pair separation of A) n=9 B) n=10 C) n=11 and D) n=12. The most probable distance agrees within 2 Å between the two.

Distance distribution from MD simulations at different time intervals

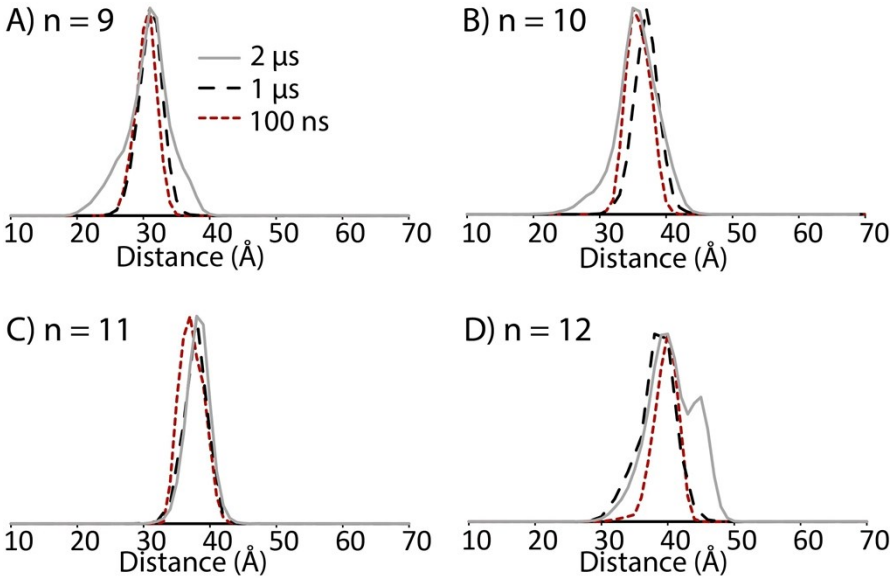

Figure S2: Comparison of distance distributions from initial 100 ns (red), initial 1 μs (black) and 2 μs (grey) simulations for duplexes with base pair separation of A) n=9 B) n=10 C) n=11 and D) n=12. The most probable distance of the three distributions agree within 2 Å.

Analysis of angle of natural base with respect to the DNA backbone

We performed molecular dynamics (MD) simulations on an unlabeled DNA duplex. The duplex has the same sequence as the labeled DNA, except the Cu^{2+}-DPA and dSpacer sites were replaced by adenine and thymine, respectively. The DNA was created using the Nucleic Acid Builder (NAB) module in the AMBER suite[1]. The duplex was then solvated in an explicit 12 Å water box using the TIP3P water model[2]. Na^+ and Cl^- ions were then added to neutralize the system. All simulations were performed using the pmemd program in the AMBER16 software package[3] and using the AMBER parmbsc1 (bsc1) force field[4]. The solvated system was optimized, thermalized and pre-equilibrated for 2 ns before initiating the unrestrained production MD run of 1 µs at 298.15 K. Periodic boundary conditions along with particle mesh ewald (PME)[5] were applied to account for long-range electrostatic interactions under NPT (P=1 atm) conditions. SHAKE[6] was then used to restrain on bonds involving hydrogens along with an integration step of 2 fs and a nonbonded cut-off of 10 Å. All visualizations of the simulations were done on VMD[7]. From the MD trajectories, angle between a natural base and the DNA backbone was analyzed. We considered the angle between the C4' atom of base *i*, C4' atom of base *i+1* and the atom at the interior of the base *i+1*.

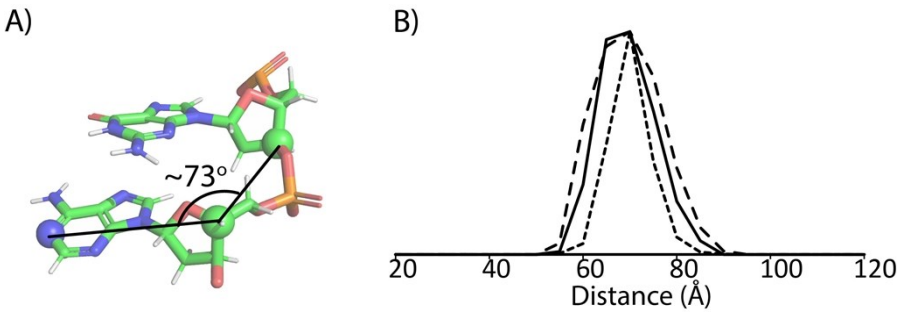

Figure S3: A) Angle between C4' atom of base *i*, C4' atom of base *i+1* and atom of base *i+1* present at the interior of the duplex. B) The angle, measured between 3 different consecutive bases (represented by solid, dashed, and dotted lines), give a most probable angle of ~ 73°.

Calculation of Cu^{2+}-proton distance from HYSCORE spectrum

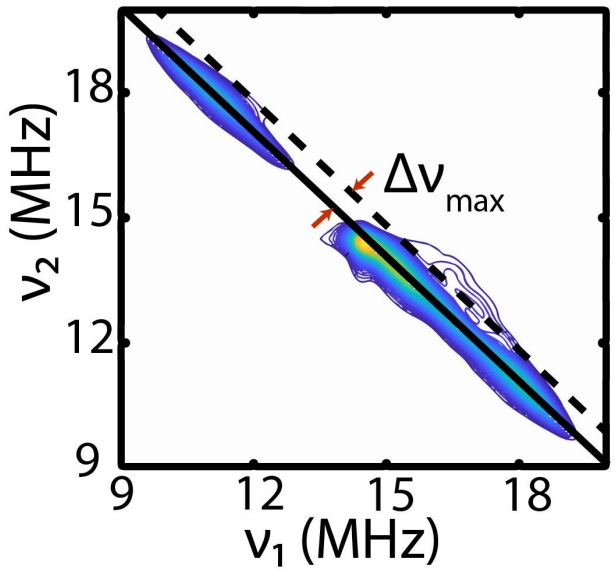

Figure S4: HYSCORE spectrum of Cu^{2+}-DPA-DNA duplex. The solid black line shows the anti-diagonal, and the red arrows indicate the maximum shift from the anti-diagonal, denoted as $\Delta\nu_{max}$.

In order to estimate Cu^{2+}-water bond length, we calculated the maximum shift from the anti-diagonal, $\Delta\nu_{max}$ in the HYSCORE spectrum. The value of $\Delta\nu_{max}$ (shown in Figure S4) was found to be 1.5 MHz. The dipolar coupling constant, T, using the equation is given by[8]

$$T = \frac{4}{3}\sqrt{\frac{2\nu_I \Delta\nu_{max}}{\sqrt{2}}}$$

where ν_I is the nuclear Larmor frequency.

Using the above equation, we obtained T = 5.1 MHz. Previous HYSCORE studies have shown that T for protons of equatorially coordinated water have a value of 4.8-5.2 MHz[9,10]. Finally, we calculated the distance between Cu^{2+}-H using the following equation[11]:

$$T = \frac{\mu_0}{4\pi} g_e g_n \beta_e \beta_n \frac{1}{r^3}$$

Applying the above equation and using our calculated T value, we obtained a Cu^{2+}-H distance of ~2.5 Å. The DFT-optimized structure yielded an average value of 2.4 Å for the two protons on the equatorially coordinated water molecule. Thus, the HYSCORE results agree well with the DFT-structure.

References

1 D. A. Case, T. E. Cheatham III, T. Darden, H. Gohlke, R. Luo, K. M. Merz Jr., A. Onufriev, C. Simmerling, B. Wang and R. J. Woods, The Amber biomolecular simulation programs, *J. Comput. Chem.*, 2005, **26**, 1668–1688.

2 W. L. Jorgensen, J. Chandrasekhar, J. D. Madura, R. W. Impey and M. L. Klein, Comparison of simple potential functions for simulating liquid water, *J. Chem. Phys.*, 1983, **79**, 926–935.

3 D. Case, R. Betz, W. Botello-Smith, D. Cerutti and T. Darden, Amber 16, *Univ. California, San Fr.*

4 I. Ivani, P. D. Dans, A. Noy, A. Pérez, I. Faustino, A. Hospital, J. Walther, P. Andrio, R. Goñi, A. Balaceanu, G. Portella, F. Battistini, J. L. Gelpí, C. González, M. Vendruscolo, C. A. Laughton, S. A. Harris, D. A. Case and M. Orozco, Parmbsc1: a refined force field for DNA simulations, *Nat. Methods*, 2016, **13**, 55–58.

5 T. Darden, D. York and L. Pedersen, Particle mesh Ewald: An $N \cdot \log(N)$ method for Ewald sums in large systems, *J. Chem. Phys.*, 1993, **98**, 10089–10092.

6 J. P. Ryckaert, G. Ciccotti and H. J. . Berendsen, Numerical integration of the cartesian equations of motion of a system with constraints: molecular dynamics of n-alkanes, *J. Comput. Phys.*, 1977, **23**, 327–341.

7 W. Humphrey, A. Dalke and K. Schulten, VMD: Visual molecular dynamics, *J. Mol. Graph.*, 1996, **14**, 33–38.

8 P. M. Schosseler, B. Wehrli and A. Schweiger, Complexation of Copper(II) with Carbonate Ligands in Aqueous Solution: A CW and Pulse EPR Study, *Inorg. Chem.*, 1997, **36**, 4490–4499.

9 C. S. Burns, E. Aronoff-Spencer, C. M. Dunham, P. Lario, N. I. Avdievich, W. E. Antholine, M. M. Olmstead, A. Vrielink, G. J. Gerfen, J. Peisach, W. G. Scott and G. L. Millhauser, Molecular features of the copper binding sites in the octarepeat domain of the prion protein, *Biochemistry*, 2002, **41**, 3991–4001.

10 M. G. Santangelo, A. Medina-Molner, A. Schweiger, G. Mitrikas and B. Spingler, Structural analysis of Cu(II) ligation to the 5′-GMP nucleotide by pulse EPR spectroscopy, *J. Biol. Inorg. Chem.*, 2007, **12**, 767–775.

11 S. Maurelli, M. Ruszak, S. Witkowski, P. Pietrzyk, M. Chiesa and Z. Sojka, Spectroscopic CW-EPR and HYSCORE investigations of Cu2+ and O2- species in copper doped nanoporous calcium aluminate (12CaO·7Al2O3), *Phys. Chem. Chem. Phys.*, 2010, **12**, 10933–10941.